

Free-Editor: Zero-shot Text-driven 3D Scene Editing

Nazmul Karim¹, Umar Khalid¹, Hasan Iqbal², Jing Hua², Chen Chen¹

¹University of Central Florida ²Wayne State University

mdnazmul.karim@ucf.edu, umar.khalid@ucf.edu, hasan.iqbal.cs@wayne.edu,

jinghua@wayne.edu, chen.chen@crcv.ucf.edu

<https://free-editor.github.io/>

Abstract

Text-to-Image (T2I) diffusion models have gained popularity recently due to their multipurpose and easy-to-use nature, e.g. image and video generation as well as editing. However, training a diffusion model specifically for 3D scene editing is not straightforward due to the lack of large-scale datasets. To date, editing 3D scenes requires either re-training the model to adapt to various 3D edited scenes or design-specific methods for each special editing type. Furthermore, state-of-the-art (SOTA) methods require multiple synchronously edited images from the same scene to facilitate the scene editing. Due to the current limitations of T2I models, it is very challenging to apply consistent editing effects to multiple images, i.e. multi-view inconsistency in editing. This in turn compromises the desired 3D scene editing performance if these images are used. In our work, we propose a novel training-free 3D scene editing technique, FREE-EDITOR, which allows users to edit 3D scenes without further re-training the model during test time. Our proposed method successfully avoids the multi-view style inconsistency issue in SOTA methods with the help of a “single-view editing” scheme. Specifically, we show that editing a particular 3D scene can be performed by only modifying a single view. To this end, we introduce an Edit Transformer that enforces intra-view consistency and inter-view style transfer by utilizing self- and cross-attention, respectively. Since it is no longer required to re-train the model and edit every view in a scene, the editing time, as well as memory resources, are reduced significantly, e.g., the runtime being $\sim 20\times$ faster than SOTA. We have conducted extensive experiments on a wide range of benchmark datasets and achieve the diverse editing capabilities with our proposed technique.

1. Introduction

Neural Radiance Fields (NeRF) [35], neural implicits [58] as well as subsequent work [30, 36, 56], collectively termed

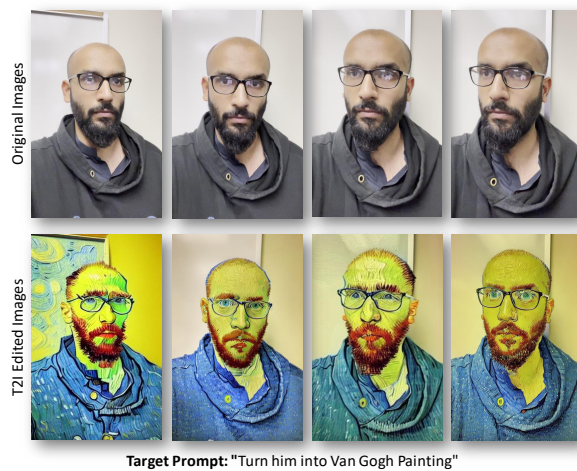


Figure 1. **Multi-View Inconsistency in Current Text-to-Image (T2I) Editing Models:** The current T2I editing model [6] faces significant challenges with multi-view consistency. This issue adversely affects the quality of 3D scene editing, especially when these edited views are used to synthesize novel views. This specific limitation is also acknowledged in InstructN2N [18]. It is important to note that this inconsistency is particularly problematic when rendering is performed *without re-training*, which aligns with the objectives of our study.

as *neural fields*, have emerged as powerful 3D neural representations. Recent advances in this field [10, 11, 36, 55, 68] have focused on both novel view synthesis, scene reconstruction as well as 3D scene manipulations such as color editing [27, 55], scene composition [52, 54], and style transfer [16, 21]. Notably, it has been shown that text-guided 3D NeRF [18, 68] editing can be achieved through leveraging the diverse generation capability of 2D text-to-image (T2I) diffusion models [6, 17, 44]. Despite their demonstrated success existing methods need to **i)** re-train the editing model for each particular 3D scene which introduces computational and memory overhead, and **ii)** rely on the prior knowledge of specific editing types, which may not be feasible in most scenarios. For instance, InstructN2N [18] iteratively edits the training images of a scene until it obtains the desired editing result of the scene. The iterative

| Methods | Re-Training | Text-Driven | Style Transfer |
|-------------------|-------------|-------------|----------------|
| Blend-NeRF [25] | ✓ | ✗ | ✗ |
| Blended-NeRF [15] | ✓ | ✓ | ✓ |
| DreamEditor [68] | ✓ | ✓ | ✓ |
| NeRF-Art [57] | ✓ | ✓ | ✓ |
| Instruct-N2N [18] | ✓ | ✓ | ✓ |
| Ours | ✗ | ✓ | ✓ |

Table 1. **Comparison with SOTA methods.** Unlike prior works, our proposed method does not re-train the model each time we have to edit a new scene.

editing is inevitable since all training images may not have consistent style information during initial iteration phase. This is due to the current limitations of T2I diffusion models as achieving prompt-consistent edits in multiple images (even if they are from the same scene) is very challenging. Fig. 1 shows an example, the same target prompt results in different multi-view outcomes within the scene. With such inconsistent edits or styles, poor 3D editing performance would be obtained even with extensive re-training. To tackle this issue of *multi-view style inconsistency*, InstructN2N requires to constantly update the training set (with suitably edited images) based on direct feedback from the model.

If we want to achieve the same goal of InstructN2N [18] without re-training, we do not get the chance to update the training set more than once. This will lead to poor performance due to the aforementioned reasons. In our work, we tackle the problem of *text-driven 3D scene editing* from a fresh perspective that alleviates the aforementioned issues. Given a 3D scene data that contains multiple source view images with their pose information, we first randomly select a view, “*starting view*”. We aim to obtain the desired 3D editing outcomes by editing only this starting view. By editing only one image view per scene, we eliminate the possibility of multi-view style inconsistency (Fig. 1) as well as reduce the overall editing time significantly. In addition, we address the problem of re-training with the help of a generalized NeRF (Gen-NeRF) model [46, 59] which leverages the style information in the starting view and multi-view geometry information from multiple non-edited source views to render a novel target view; which have the same style as the starting view. Due to the generalization power of Gen-NeRF, we can perform zero-shot 3D scene editing by introducing some key architectural design changes.

However, there are some challenges associated with this: *First*, transferring style information from the starting view to the target view requires the view geometry correspondence information. In our framework, the view-geometry correspondence is solved by leveraging pixel-aligned features for each target pixel. To further enhance these features (obtained from non-edited source views) with style information, we utilize an *Edit Transformer (ET)* that employs both self- and cross-attentions. With self-attention, it

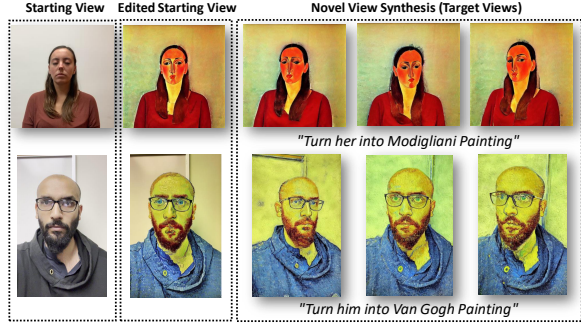


Figure 2. **Novel View Synthesis** using our proposed method for different target poses.

can grasp long-range content information within the starting view. On the other hand, it can enrich the pixel-aligned features with content details from the starting view with the help of cross-attention. Subsequently, these style-informed features (obtained from ET) are converted into RGB color using another transformer. *Second*, features obtained from ET lack necessary spatial awareness as closely situated neighboring views from the same scene should change continuously. This may lead to spatial non-smoothness in the pixel space which is highly undesirable for a style transfer. To circumvent this, we design a multi-view consistency loss that enforces the features at two spatially close points to be similar. In addition, *self-view robust loss* is proposed to encourage consistent color rendering in the final synthesized target view.

Our main contributions can be summarized as follows:

- We propose FREE-EDITOR, a zero-shot text-guided 3D scene editing technique that can synthesize novel views based on a text description while maintaining high 3D consistency. With the help of a generalized NeRF model, our unique method avoids the need for scene-specific re-training or adaptation across various editing styles.
- Our proposed method successfully avoids the *multi-view style inconsistency* issue in SOTA methods with the help of a “single-view editing” scheme. It allows to edit a particular 3D scene by only modifying a single view (see Fig. 2) since our designed *Edit Transformer* enforces intra-view consistency and inter-view style transfer by utilizing self- and cross-attention, respectively.
- Due to the unique design choices in FREE-EDITOR, both training costs as well as editing time are reduced significantly. We tested various editing styles on multiple datasets extensively to demonstrate its superiority.

2. Related Work

Novel View Synthesis With NeRF. was first introduced in [35], generates realistic novel views by fitting scenes as continuous 5D radiance fields using a Multilayer Perceptron (MLP). Since its inception, several advancements have enhanced NeRFs. For instance, Mip-NeRF [4, 5] effi-

ciently handles object scale in unbounded scenes. Nex [61] models significant view-dependent effects whereas other works [37, 58] improve surface representation, extend to dynamic scenes [39], etc. Despite the tremendous success of NeRF, its time-consuming per-scene fitting poses a notable drawback. To address this, Generalizable NeRFs aim to bypass this optimization hurdle by framing new view creation as an image-based interpolation challenge across different views. Approaches like NeuRay [32], IBRNet [60], MVSNerF [8], and PixelNeRF [65] construct a universal 3D representation using combined features from observed views. GPNR [51] and GNT [59] elevate the quality of generated new views through a Transformer-based aggregation method. In our work, we also consider Generalized NeRF as we do not aim to re-train the model.

Diffusion-based 2D Image Editing. Text-guided image synthesis has garnered substantial attention within the generative model domain [1–3, 14, 38, 62, 66]. Recent advancements in diffusion models ([48, 49]) have presented innovative approaches, yielding impressive outcomes [42, 43, 45]. With significant enhancements in this domain, the focus has been shifted from training extensive text-to-image models from scratch to leveraging open-source pre-trained models for prompt-guided image manipulation [13, 20, 24, 31]. These text-driven editing techniques serve diverse purposes like image editing, style transfer, and generator domain adaptation [17, 28, 44, 50, 63, 67].

Diffusion-based 3D Scene Editing. The emergence of text-to-image conversion models has notably impacted NeRF editing. Beginning with the Score Distillation Sampling method in DreamFusion [40], Vox-e [47] explored techniques to regulate alterations in pre-existing voxel fields. NeRF-Art [57] utilizes various regularization approaches during training to ensure that NeRF when edited using CLIP, preserves the original structure. InstructNerf2Nerf (IN2N) (Instruct-NeRF2NeRF) employed 2D image translation models [18] to adjust 2D image characteristics for NeRF training based on textual prompts. However, IN2N’s reliance on IP2P [6] for updating NeRF training data tends to excessively modify scenes. Furthermore, encounter difficulties such as extended training durations and unstable loss functions. Addressing the challenge of undesired alterations, DreamEditor [68] introduced a mesh-based neural field that efficiently converts 2D masks into 3D editing areas. This enables precise local modifications while avoiding unnecessary geometric changes when altering only the appearance. Similarly, Blended-NeRF [15] and Blend-NeRF [25] require additional cues like bounding boxes for localized editing. However, all of these methods require per-scene adaptation of the 3D model to induce any editing effects which increases computational overhead significantly. In our work, we propose a zero-shot editing

technique that performs similarly or better than SOTA and is more practically applicable.

3. Method

3.1. Background

Neural Radiance Fields. In neural radiance fields (NeRF) [35], the task is to find a neural network based representation of 3D scenes. The neural network here is a multi-layer perceptron (MLP) that maps a 3D location $\mathbf{x} \in \mathbb{R}^3$ and viewing direction $\mathbf{d} \in \mathbb{S}^2$ to an emitted color $\mathbf{c} \in [0, 1]^3$ and a volume density $\sigma \in [0, \infty)$,

$$\mathcal{F}(\mathbf{x}, \mathbf{d}; \Theta) \mapsto (\mathbf{c}, \sigma), \quad (1)$$

where \mathcal{F} and Θ represent the MLPs and the set of learnable parameters, respectively. where \mathcal{F} is the MLPs, and Θ is the set of learnable parameters of NeRF.

Volume Rendering. Let us define $\mathbf{r}(t) = \mathbf{o} + t\mathbf{d}$ as a ray in a NeRF, where \mathbf{o} is the camera center and \mathbf{d} is the ray’s unit direction vector. Along this ray, we can predict the color values \mathbf{c}_i and volume densities σ_i of K sample points, $\{\mathbf{r}(t_i) | i = 1, \dots, K\}$, by following this formal procedure:

$$\hat{\mathbf{C}}(\mathbf{r}) = \sum_{i=1}^K w_i \mathbf{c}_i, \quad \text{where} \quad (2)$$

$$w_i = \exp\left(-\sum_{j=1}^{i-1} \sigma_j \delta_j\right) (1 - \exp(-\sigma_i \delta_i)).$$

Here, w_i indicates the weight or hitting probability of i -th sampling point [32] and δ_i is the distance between adjacent samples.

3.2. Free-Editor: 3D Scene Editing

In this section, we present our proposed method, *Free-Editor*, that enables training-free editing of a 3D Scene. Consider a dataset that contains L number of 3D scenes in terms of images and their camera intrinsic and extrinsic parameters. Let us define a 3D scene training data that contains N images with their corresponding camera parameters, $\{I_l \in \mathbb{R}^{H \times W \times 3}, P_l \in \mathbb{R}^{3 \times 4}\}$. First, we select a “starting view” I_0 and render a “target view” I_t . To apply specific 2D editing in I_t and I_0 , we employ a text-guided diffusion model \mathbf{D} with group attention,

$$\hat{I}_0 = \mathbf{D}(I_0, C_{in}^0, C_{tgt}^0, \Phi), \hat{I}_t = \mathbf{D}(I_t, C_{in}^t, C_{tgt}^0, \Phi), \quad (3)$$

where Φ is the diffusion model, C_{in}^0 and C_{in}^t are the input captions of I_0 and I_t , respectively. On the other hand, C_{tgt}^0 is the target caption that will perform the editing. We employ group attention to have consistent editing results in \hat{I}_0 and \hat{I}_t . This is very important as the final 3D editing results

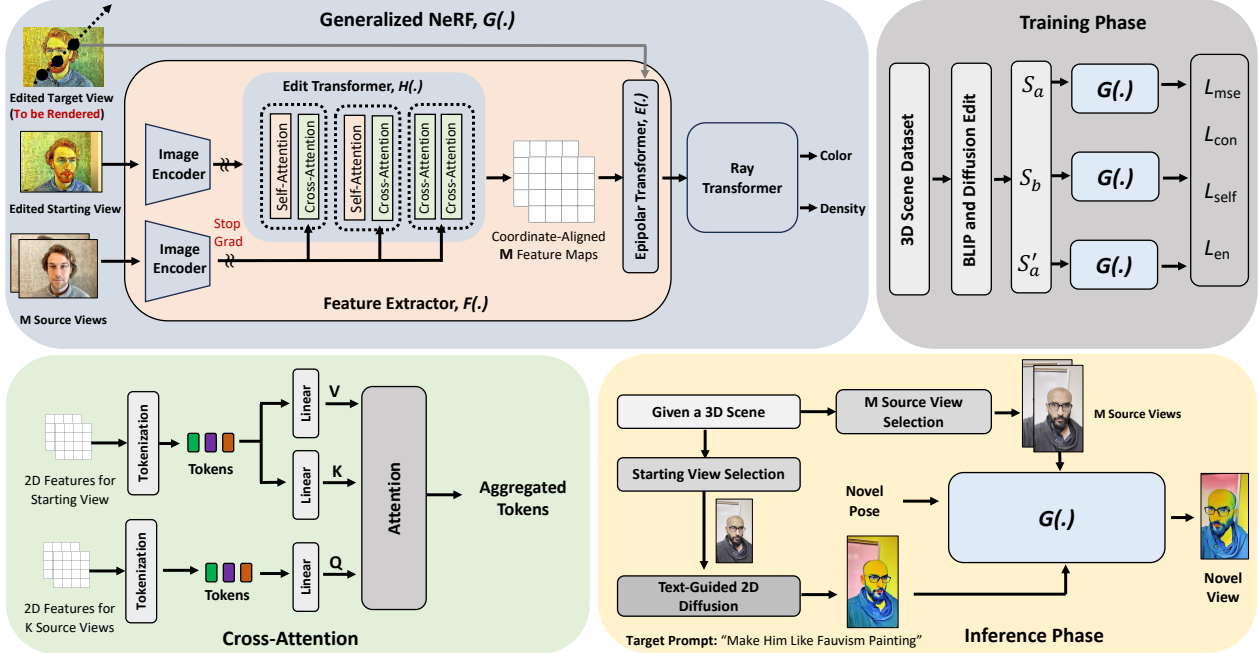


Figure 3. **Overview of our proposed method.** *Top Left.* We train a generalized NeRF ($G(\cdot)$) that takes a single edited starting view and M source views to render a novel target view. Here, "Edited Target View" is not the input to the model rather will be rendered and works as the ground truth for the prediction of $G(\cdot)$. In $G(\cdot)$ we employ a special *Edit Transformer* that utilize: *Bottom Left.* cross-attention to produce style-informed source feature maps that will be aggregated through an Epipolar Transformer. *Top Right.* During training, we employ different sets of source views S_a, S_b, S'_a for 4 different loss functions we used for training. Note that S'_a is a variant of S_a with additional ray information for calculating L_{con} . *Bottom Right.* During Inference, only a single image needs to be edited to obtain a 3D edited NeRF.

depend largely on this. More about this is in the [supplementary](#).

As the next step, we perform "source-view selection" to select M source views, $S = \{I_m, P_m\}_{m=1}^M$, from the remaining source views $\{I_n, P_n\}_{n=1}^{N-1}$, where $M < N - 1$. In Sec. 3.2.3, we explain how to select these views in detail. The generalized NeRF model [23, 32] with parameters θ , $G(\cdot; \theta)$, takes $\{I_m, P_m\}_{m=1}^M$ and \hat{I}_0, P_0 as inputs and predicts \tilde{I}_t as output,

$$\tilde{I}_t = G(\hat{I}_0, I_m, P_0, P_m, \theta | m = 1, \dots, M) \quad (4)$$

Our objective is to train $G(\cdot; \theta)$ by minimizing the following optimization objective,

$$\arg \min_{\theta} \|\hat{I}_t - \tilde{I}_t\|^2. \quad (5)$$

3.2.1 Style-aware Multi-view Feature Extraction

In Figure 3, we show the details of our proposed method. We can consider the generalized NeRF as a combination of feature extractor (F) to extract coordinate-aligned feature maps before aggregating them and ray transformer (R) [59] that will transform the features into color and density. Using F , we adopt a feed-forward fashion to extract generalized features from multi-view images $\hat{I}_0, \{I_m, P_m\}_{m=1}^M$ and convert them later into 3D representation using R . In

eq. 1, we show how a 3D location can be mapped into color and density. Here, we do that in two stages: i) create a coordinate-aligned feature field using F , and ii) aggregate point-wise features along different rays to form ray colors using an attention-based ray transformer. We use \hat{I}_t as the ground truth for ray colors.

We first construct hierarchical image features using pre-trained 2D CNN Image Encoder [19] as follows, $f_i = T(I_i); m = 1, \dots, M$, where f_i is the image feature for i^{th} source image. We then feed these features to the newly proposed edit transformer, $h_i = H(\hat{f}_0, f_i)$, which would give us the editing-informed multi-view feature maps. Here, \hat{f}_0 is the 2D image feature corresponding to the starting view, \hat{I}_0 . We use both self-attention and cross-attention in our edit transformer (shown in Fig. 3) with different purposes. The functional mechanism of attention can be defined as $\text{Attention}(Q, K, V) = \text{Softmax}(\frac{QK^T}{\sqrt{d}}) \cdot V$, where

$$Q = W^Q z, K = W^K z, V = W^V z. \quad (6)$$

Here, W^Q, W^K , and W^V denote trainable matrices that project the inputs to the query (Q), key (K), and value (V) components, respectively. z represents the latent features, and d represents the output dimension of the key and query features. The objective of self-attention is to learn long-range and relevant information within a given view. In our particular case, we aim to capture the exact editing effects

that have taken place in \hat{I}_0 utilizing self-attention. However, capturing only single-view information using self-attention is not enough as it is required to have multi-view feature maps for a successful novel view synthesis. To understand why multi-view information is needed, we briefly analyze the recently proposed Epipolar Aggregated Transformer [51, 64] which functions between the target pixels and pixels positioned on the epipolar line of multiple source views. Using the epipolar geometry constraint, the features can be aggregated to capture long-range content information within and across images. However, vanilla multi-view feature maps obtained from M source views do not have the editing information in \hat{I}_0 . We find a simple fix to this issue by explicitly injecting editing information from \hat{I}_0 into the multi-view source feature maps with the help of cross-attention. As shown in Fig. 3, we first tokenize the 2D image features obtained from T which reduces the attention complexity significantly. To extract the key (K) and value (V), tokens from the starting view are used whereas we use source views tokens as the query (Q). Using cross-attention, we aggregate features from source views towards the root of the editing effects, \hat{I}_0 .

Now, for each target pixel in \hat{I}_t , we uniformly sample P coordinate-aligned 3D points $\{\mathbf{x}_1, \dots, \mathbf{x}_P\}$ from the set of points between far and near planes. Each of these points is projected into the feature maps obtained from H and then aggregated to form a coordinate-aligned feature field as follows,

$$\mathbf{F}(\mathbf{x}_p, \phi) = \mathbf{E}(\mathbf{h}_1(\Pi_1(\mathbf{x}_p)), \dots, \mathbf{h}_M(\Pi_M(\mathbf{x}_p))). \quad (7)$$

Here, \mathbf{E} is the Epipolar Aggregated Transformer, $\Pi_i(\mathbf{x}_p)$ projects 3D point \mathbf{x}_p onto the i -th source-image plane with the help of an extrinsic matrix. We use bilinear interpolation to compute the feature vector $\mathbf{h}_1(\mathbf{u})$ at projected 2D position $\mathbf{u} \in \mathbb{R}^2$. Finally, we utilize the Ray Transformer \mathbf{R} along with an MLP to dynamically learn the blending weights along the ray for each point and produce the RGB color information. Given ray information, \mathbf{r} and $\{\mathbf{x}_1, \dots, \mathbf{x}_P\}$ as the uniformly sampled points along \mathbf{r} , an MLP (\mathbf{V}) can be used to map the pooled features vectors from \mathbf{R} to RGB color \bar{C}_t ,

$$\bar{C}_t(\mathbf{r}) = \mathbf{V}(\mathbf{R}(\mathbf{F}(\mathbf{x}_p, \phi))); p \in [1, P]. \quad (8)$$

3.2.2 Loss Functions

For training the model end-to-end, we employ different loss functions that serve important roles in producing good performance.

Photometric Loss, L_{mse} . First, we adopt the photometric loss in NeRF [35] which is defined as the mean square error

(MSE) between the predicted and ground truth pixel colors,

$$L_{mse} = \sum_{\mathbf{r} \in \mathcal{R}} \|\bar{C}_t(\mathbf{r}) - C_t(\mathbf{r})\|^2, \quad (9)$$

where \mathcal{R} represents the set of rays and $C_t(\mathbf{r})$ is the ground truth pixel values in \hat{I}_t for ray $\mathbf{r} \in \mathcal{R}$.

Multi-view Consistency Loss, L_{con} . In our work, we proposed to edit only a single image to reconstruct an edited 3D scene. Due to the nature of our problem formulation, achieving spatial smoothness is challenging due to the constraints of view geometry in NeRF. Although we use cross-attention to induce the editing effects in the feature maps, it is necessary to set an objective function that would encourage multi-view consistency among the features. This in turn leads to a smooth transition between texture or color between neighboring views. Let us denote $e_p^j = \{\mathbf{h}_1(\Pi_1(\mathbf{x}_p^j)), \dots, \mathbf{h}_M(\Pi_M(\mathbf{x}_p^j))\}$ as the feature distribution obtained at 3D point \mathbf{x}_p^j using the features from M source views. Here, j indicates that \mathbf{x}_p^j is sampled along the ray, \mathbf{r}_j . Let us select another ray $\mathbf{r}_{j'}$ which can be either very close to \mathbf{r}_j or a slightly perturbed version of \mathbf{r}_j . For each point \mathbf{x}_p^j , we select its closest point $\mathbf{x}_p^{j'}$ along ray j' based on their Euclidean distance, denoted as $d_{j,j'}^p = \|\mathbf{x}_p^j - \mathbf{x}_p^{j'}\|$. Therefore, we encourage consistency among the coordinate-aligned features of the closest points with the help of Jensen-Shannon Divergence (JSD) loss,

$$L_J(\mathbf{x}_p) = D_{JSD}(e_p^j, e_p^{j'}), \quad (10)$$

where $e_p^{j'}$ is the features corresponding to $\mathbf{r}_{j'}$. We use JSD loss for its symmetric nature which offers some notable advantages over Kullback–Leibler (KL) divergence [22] loss. Since closer points in the pixel space should have smaller distances in the feature space, we employ a weighted JSD loss for defining our final multi-view consistency loss,

$$L_{con} = \sum_{p=1}^P \omega_p L_{JSD}(\mathbf{x}_p). \quad (11)$$

Here, ω_p indicates the weight corresponding to the pair $(\mathbf{x}_p^j, \mathbf{x}_p^{j'})$ which can be expressed as $\omega_p = \frac{e^{-d_{j,j'}^p}}{\sum_{p=1}^P e^{-d_{j,j'}^p}}$.

Our unique formulation of L_{con} imposes consistency on 3D points across various viewpoints, inherently promoting smoothness in the scene’s geometry.

Self-View Robust Loss, L_{self} . In general, when the training data for a 3D scene remains coherent, generating the same target view using different source views usually produces consistent outcomes. However, this may not hold true for our case as we are dealing with an edited target view. To address this, we choose two different sets of source views

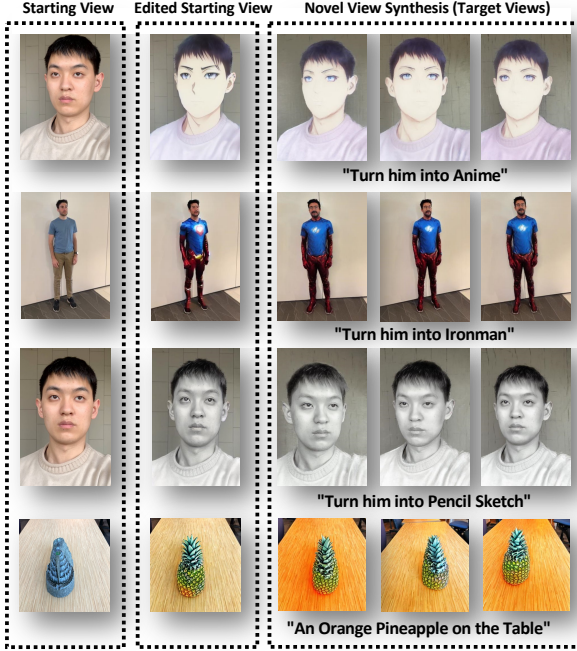


Figure 4. **Text-driven 3D scene editing.** Illustration of text-driven 3D scene editing using our proposed method across various target poses. This figure showcases the view-consistent results generated by our method. A qualitative evaluation on multiple scenes reveals the efficacy of our approach: starting from a single view, our method successfully generates novel views that are conditioned on the editing prompt, demonstrating its robustness and versatility in 3D scene editing.

$S_a = \{I_m^a, P_m^a\}_{m=1}^M$ and $S_b = \{I_m^b, P_m^b\}_{m=1}^M$. The predicted target views utilizing S_a and S_b are \hat{I}_t^a and \hat{I}_t^b , respectively which should have consistent content information. To ensure this consistency, we employ

$$L_{self} = \sum_{r \in \mathcal{R}} \|\bar{C}_t^a(r) - \bar{C}_t^b(r)\|^2, \quad (12)$$

where \bar{C}_t^a and \bar{C}_t^b indicate RGB color values in \hat{I}_t^a and \hat{I}_t^b , respectively.

Entropy Loss, L_{en} . In addition, we consider an entropy loss for regularizing the hitting probabilities of the sampled points [26],

$$L_{en} = - \sum w_i \log(1 - w_i). \quad (13)$$

Finally, the total loss function employed to train our framework can be expressed as follows,

$$L_{tot} = L_{mse} + \lambda_c L_{con} + \lambda_s L_{self} + \lambda_e L_{en}, \quad (14)$$

where $\lambda_c, \lambda_s, \lambda_e$ are the loss coefficients.

3.2.3 Training and Inference Phase

Training Data Generation and View Selection. To generate the training data, we utilize the open-source pre-trained

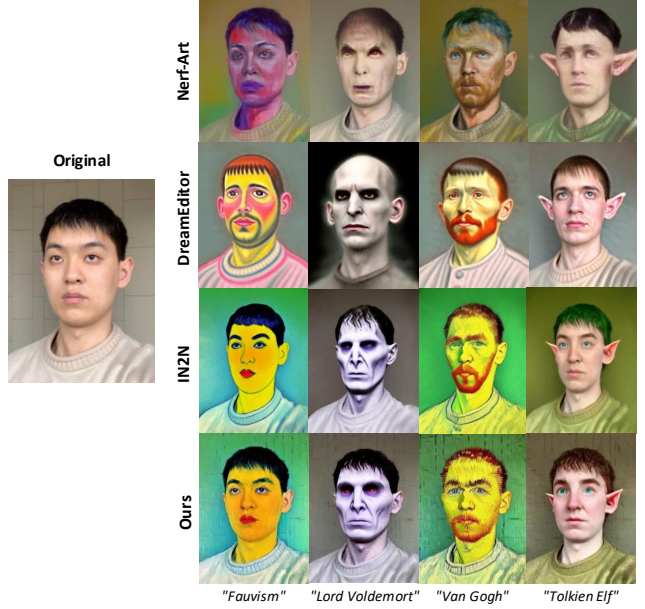


Figure 5. **Style Transfer.** Exhibiting the proficiency in conducting style edits within 3D NeRF Scenes, our method exemplifies its versatility and precision through intricate modifications and advanced prompt-guided editing in a three-dimensional environment. Visually, our outcomes bear a resemblance to those of IN2N, since both methods utilize IP2P for 2D image editing. However our method tends to preserve background details more effectively than IN2N.

models BLIP [29] and Instruct-Pix2Pix [6] text-guided diffusion model. For generating the input caption C_{in}^0 of starting view image I_0 , we use BLIP model before modifying it to C_{tgt}^0 using a GPT [7] model. Finally, we feed C_{tgt}^0 and I_0 to Instruct-Pix2Pix to produce \hat{I}_0 . We do the same for generating \hat{I}_t . Note that, we generate multiple copies of \hat{I}_t and make sure the editing is consistent with the \hat{I}_0 using CLIP score. For a particular scene, we repeat this process multiple times and select a new starting view in each iteration. For *source-view selection*, we select M (= 12) views that are spatially close to the *starting view* \hat{I}_0 .

Inference Phase. During inference, we randomly select a starting view image that will be edited and M non-edited source images following the criterion *source-view selection*. Now, we can simply render an edited target view by providing novel target pose information to the model.

4. Experiments and Analysis

Datasets. Our model is trained on datasets including Google Scanned Objects [9], NerfStudio [53] NeRF-Synthetic [34], Spaces [12], and IBRNet-collect [60]. For evaluation, we use IN2N [18], NeRF-Art [57], LLFF [33], and our own dataset comprising four scenes.

Baselines. We report qualitative and quantitative comparisons against four baseline NeRF editing methods in-

| Metrics | CLIP-NeRF | NeRF-Art | Instruct N2N | DreamEditor | Ours |
|-----------|-----------|----------|---------------|-------------|--------------|
| Edit PSNR | 22.15 | 20.89 | 22.16 | 22.34 | 22.47 |
| CTDS | 0.2375 | 0.2503 | 0.2804 | 0.2788 | 0.2601 |
| CDC | 0.9672 | 0.9751 | 0.9882 | 0.9850 | 0.9781 |

Table 2. **Quantitative assessment of 3D scene editing focusing on text alignment and frame consistency** is conducted. Our method exceeds all other state-of-the-art editing techniques in terms of Edit PSNR metric while achieving comparable performances in other scenarios.

| Method | LLFF | LLFF-P | Use Cases | w/o L_{con} | w/o L_{self} | All Loss |
|--------------------|--------------|--------------|-----------|---------------|----------------|--------------|
| PixelNeRF | 18.66 | 11.03 | Case 1 | 20.98 | 19.63 | 22.76 |
| MVSNeRF | 21.18 | 16.74 | Case 2 | 22.86 | 21.52 | 23.11 |
| IBRNet | 25.17 | 20.05 | Case 3 | 23.14 | 22.29 | 24.21 |
| Neuray | 25.35 | 19.31 | Case 4 | 23.08 | 21.81 | 23.96 |
| GeoNeRF | 25.44 | 19.98 | Case 5 | 21.37 | 20.13 | 22.56 |
| FREE-EDITOR (Ours) | 23.81 | 22.54 | Case 6 | 21.25 | 20.38 | 22.03 |

Table 3. **Comparison of Mean PSNR** with recent SOTA generalized NeRF methods as we are also employing a generalizable model for scene editing.

Table 4. **Quantitative ablation study** with different loss functions. Self-view robust loss impacts the color consistency while L_{con} impacts the smooth transfer of color information.

cluding IN2N [18], NeRF-Art [57], CLIP-NeRF [55], and DreamEditor [68]. The default 2D-image editing model is Instruct-Pix2Pix (IP2P) [6]

4.1. Qualitative Results

Figures 4, 5 demonstrate the proficiency of our method in executing effective style edits, maintaining 3D coherence, and conforming to textual narratives.

Text-driven 3D Scene Editing. Figure 4 shows the text-driven editing performance of our proposed method. We use different text-scene pairs to show the diversity of our method. We start with the edited starting view and produce the novel target view from different poses. Our method shows notable alignment between the provided text description and the resulting views. Yet, there are instances where the alignment isn’t perfect. For instance, when attempting to transform an image into an anime style, the details around the nose might not be accurately captured. This kind of intricate detail can be challenging to represent when working within significant limitations during the editing process. More on this is in [supplementary](#).

Style Transfer. Figure 5 illustrates the visual comparisons between FREE-EDITOR and other 3D scene style transfer methods. Owing to the use of the IP2P [6] editing backbone, our editing outcomes closely resemble those of IN2N [18]. However, the distinct advantage of our approach lies in its training-free nature, setting it apart from others. A notable distinction is that our method tends to preserve background details more effectively than IN2N [18], which often struggles to maintain this aspect. Comparisons with top-tier methods further corroborate the effectiveness of our technique and show the adeptness of our method in capturing both the color palette and stroke patterns of the desired

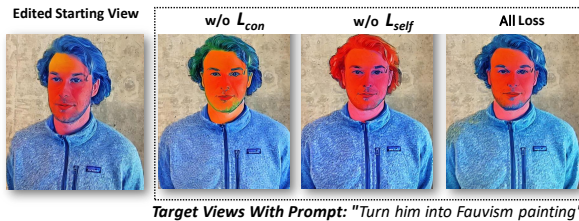


Figure 6. **Loss Sensitivity.** An ablation study focusing on the proposed loss functions sensitivity, demonstrating the effectiveness of our proposed optimization algorithm.

style. Furthermore, our results are more realistic and preserve non-targeted areas, facilitating multiple sequential edits. Details are in [supplementary](#).

4.2. Quantitative Results

3D Scene Editing. The chosen metrics for the editing evaluation are CLIP Text-Image Directional Similarity (CTDS) and CLIP directional consistency (CDS), which serve as indicators of how effectively each method preserves 3D consistency across edited scenes. CTDS evaluates how well the executed 3D edits correspond to the text instructions. While CDS is akin to CTDS it assesses the similarity in direction between the original and edited images in successive frames along newly generated camera paths. Additionally, *Edit PSNR* compares the cosine similarity and PSNR between each rendered view from the edited NeRF and from the input NeRF. These metrics collectively provide insight into the integrity of the 3D scene post-editing.

Table 2 showcases quantitative evaluations across 15 diverse scene editing tasks. Our findings indicate that both IN2N and our proposed approach produce outcomes consistent with the original viewpoints, demonstrated by their CLIP directional scores. Notably, the proposed method outperforms IN2N in terms of Edit PSNR, signifying better preservation of scene consistency with the original input. This suggests that our method maintains the details of the initial scene while implementing edits more effectively. Despite these advantages, our method slightly lags behind IN2N in overall performance, likely due to the zero-shot nature of FREE-EDITOR. However, our findings underscore the strength of the proposed method in preserving scene integrity during editing endeavors.

Generalization to New Scenes. Although the goal of our work is scene editing, we employed a generalized NeRF to achieve zero-shot capabilities. Therefore, it necessitates us to validate our method in generalization tasks too. For this, we consider the LLFF dataset and a slightly perturbed version of this dataset, LLFF-P with minor diffusion-based editing, e.g. very minor color or attribute changes. Table 3 shows our findings for this particular experiment. For the regular LLFF dataset, FREE-EDITOR obtains slightly worse

| Method | PSNR (dB) | Edit-time (mins.) | Time Complexity | Space Complexity |
|---------------------------|--------------|-------------------|-----------------|------------------|
| Clip-NeRF | 21.15 | 1034.2 | $O(n)$ | $O(n)$ |
| NeRF-Art | 21.64 | 780.6 | $O(n)$ | $O(n)$ |
| Instruct-N2N | 22.98 | 62.1 | $O(n)$ | $O(n)$ |
| DreamEditor | 23.18 | 70.5 | $O(n)$ | $O(n)$ |
| FREE-EDITOR (Ours) | 23.06 | 3.2 | $O(n)$ | $O(1)$ |

Table 5. **Efficiency comparison of different methods.** We take 2 of our scenes and apply 10 different editing before averaging. We achieve significantly faster editing time as well as better space complexity as we are not re-training the model and editing all training images.

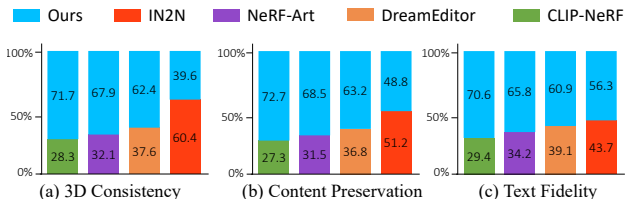


Figure 7. In an extensive **user study** that assessed three evaluation metrics, our approach demonstrated comparable performance to IN2N [18]

performance than previous methods which is somewhat understandable as it is developed mostly for scene editing. However, if we use even very minor perturbations on LLFF these methods struggle to achieve satisfactory outcomes. If the editing is more severe the performance drops even more. This shows that one can not just use an off-the-shelf generalized NeRF for editing purposes. It also shows the necessity of developing a special technique that is not just generalizable but also has editing capabilities.

4.3. Ablation Studies

In this section, we perform an ablation study with different loss functions and the efficiency of FREE-EDITOR.

Effect of Different Loss Functions. We study the impact of different loss functions on the overall performance of our proposed method. Table 4 shows 6 different use cases (scenes) where we apply 4 different text prompts for each scene. It can be observed that L_{self} has the most impact on the editing performance. The reason behind this is the compromised generalizability of the model without L_{self} . On the other hand, L_{con} helps us obtain better spatial smoothness which can be also shown by the qualitative comparison we present in Fig. 6. Note that the impact of L_{con} decreases with a larger value for a number of source views, M .

Model Efficiency. One of the main goals is to edit a particular 3D scene within a realistic timeframe. Table 5 shows that we are close to achieving that goal. FREE-EDITOR obtains almost $20\times$ better runtime efficiency as compared to the previous SOTA. Our proposed approach not only reduces the total editing time but also obtains better space efficiency, leading to a constant space complexity of $O(1)$. On the contrary, previous methods necessitate the retraining of a model for each distinct scene or editing type, resulting in increased space complexity $O(n)$.

4.4. User Study

We conducted a user study to observe the acceptability of our method in comparison to other leading-edge methods. This study involved a broad participant base, resulting in a total of 1000 responses across three critical evaluation criteria: the 3D spatial coherence, the retention of the original scene’s elements, and the accuracy in reflecting the given textual descriptions. The outcomes of this user survey are visually represented in Figure 7. These results indicate a preference for results generated by our method and IN2N [18], highlighting Free-Editor’s proficiency in these key areas. Detailed information regarding the methodology and execution of this user study is provided in the [supplementary](#).

5. Discussion and Limitations

Regarding inconsistency in multi-view edited images from the same scene, we can solve this problem through *trial and error*. Specifically, we can generate a particular set of edited images and then observe the rendering performance. Since we are using a pre-trained 2D diffusion model, we can repeat this process until we get our desired editing effects in the target view. However, it may take hundreds of *trial and error* iterations before reaching a reasonably good performance on the edited scene. Another way we can tackle the problem of *multi-view inconsistency* is to design a view-filtering system that will give us the set of edited source images with the best consistency score. For calculating this score, we can use CLIP [41] score as well as the model feedback. A good design of the filtering system can reduce the 3D inconsistency among the edited images significantly.

Although we are editing only a single image, FREE-EDITOR still depends on the 2D image pre-editing process [6] for such edits. Failures editing this single view adversely affect 3D scene editing outcomes. This is a crucial factor in our work as the success of our method heavily relies on the success of 2D editing. For this, we can use the CLIP consistency score to see whether we have a good starting view.

6. Conclusion

We have proposed a zero-shot text-driven 3D scene editing technique that does not require any re-training. Although the issue of re-training can be addressed by training a generalized NeRF model, the produced features do not contain the necessary editing information. To overcome this, our proposed edit transformer can effectively transfer the style information to the rendered target views through cross-attention. In addition, multi-view consistency loss and self-view robust loss are employed to further enhance spatial smoothness and color consistency. Our method offers not only diverse editing capabilities, but also considerable benefits in processing speed and storage

efficiency when compared with prior methods that require model retraining for individual scenes or modifications.

References

- [1] Rameen Abdal, Peihao Zhu, John Femiani, Niloy J Mitra, and Peter Wonka. Clip2stylegan: Unsupervised extraction of stylegan edit directions. corr abs/2112.05219 (2021). *arXiv preprint arXiv:2112.05219*, 2021. [3](#)
- [2] Rameen Abdal, Peihao Zhu, Niloy J Mitra, and Peter Wonka. Styleflow: Attribute-conditioned exploration of stylegan-generated images using conditional continuous normalizing flows. *ACM Transactions on Graphics (ToG)*, 40(3):1–21, 2021.
- [3] Omri Avrahami, Dani Lischinski, and Ohad Fried. Blended diffusion for text-driven editing of natural images. In *CVPR 2022*, pages 18208–18218, 2022. [3](#)
- [4] Jonathan T Barron, Ben Mildenhall, Matthew Tancik, Peter Hedman, Ricardo Martin-Brualla, and Pratul P Srinivasan. Mip-nerf: A multiscale representation for anti-aliasing neural radiance fields. In *Proceedings of the IEEE/CVF International Conference on Computer Vision*, pages 5855–5864, 2021. [2](#)
- [5] Jonathan T Barron, Ben Mildenhall, Dor Verbin, Pratul P Srinivasan, and Peter Hedman. Mip-nerf 360: Unbounded anti-aliased neural radiance fields. In *Proceedings of the IEEE/CVF Conference on Computer Vision and Pattern Recognition*, pages 5470–5479, 2022. [2](#)
- [6] Tim Brooks, Aleksander Holynski, and Alexei A Efros. Instructpix2pix: Learning to follow image editing instructions. *arXiv preprint arXiv:2211.09800*, 2022. [1](#), [3](#), [6](#), [7](#), [8](#)
- [7] Tom Brown, Benjamin Mann, Nick Ryder, Melanie Subbiah, Jared D Kaplan, Prafulla Dhariwal, Arvind Neelakantan, Pranav Shyam, Girish Sastry, Amanda Askell, et al. Language models are few-shot learners. *Advances in neural information processing systems*, 33:1877–1901, 2020. [6](#)
- [8] Anpei Chen, Zexiang Xu, Fuqiang Zhao, Xiaoshuai Zhang, Fanbo Xiang, Jingyi Yu, and Hao Su. Mvsnerf: Fast generalizable radiance field reconstruction from multi-view stereo. In *Proceedings of the IEEE/CVF International Conference on Computer Vision*, pages 14124–14133, 2021. [3](#)
- [9] Laura Downs, Anthony Francis, Nate Koenig, Brandon Kinman, Ryan Hickman, Krista Reymann, Thomas B McHugh, and Vincent Vanhoucke. Google scanned objects: A high-quality dataset of 3d scanned household items. In *2022 International Conference on Robotics and Automation (ICRA)*, pages 2553–2560. IEEE, 2022. [6](#)
- [10] Shuangkang Fang, Yufeng Wang, Yi Yang, Weixin Xu, Heng Wang, Wenrui Ding, and Shuchang Zhou. Pvd-al: Progressive volume distillation with active learning for efficient conversion between different nerf architectures. *arXiv preprint arXiv:2304.04012*, 2023. [1](#)
- [11] Shuangkang Fang, Weixin Xu, Heng Wang, Yi Yang, Yufeng Wang, and Shuchang Zhou. One is all: Bridging the gap between neural radiance fields architectures with progressive volume distillation. In *Proceedings of the AAAI Conference on Artificial Intelligence*, pages 597–605, 2023. [1](#)
- [12] John Flynn, Michael Broxton, Paul Debevec, Matthew DuVall, Graham Fyffe, Ryan Overbeck, Noah Snavely, and Richard Tucker. Deepview: View synthesis with learned gradient descent. In *Proceedings of the IEEE/CVF Conference on Computer Vision and Pattern Recognition*, pages 2367–2376, 2019. [6](#)
- [13] Rinon Gal, Yuval Alaluf, Yuval Atzmon, Or Patashnik, Amit H Bermano, Gal Chechik, and Daniel Cohen-Or. An image is worth one word: Personalizing text-to-image generation using textual inversion. *arXiv preprint arXiv:2208.01618*, 2022. [3](#)
- [14] Shijie Geng, Jianbo Yuan, Yu Tian, Yuxiao Chen, and Yongfeng Zhang. Hiclip: Contrastive language-image pre-training with hierarchy-aware attention. *arXiv preprint arXiv:2303.02995*, 2023. [3](#)
- [15] Ori Gordon, Omri Avrahami, and Dani Lischinski. Blended-nerf: Zero-shot object generation and blending in existing neural radiance fields. *arXiv preprint arXiv:2306.12760*, 2023. [2](#), [3](#)
- [16] Jiatao Gu, Lingjie Liu, Peng Wang, and Christian Theobalt. Stylenerf: A style-based 3d-aware generator for high-resolution image synthesis. *arXiv preprint arXiv:2110.08985*, 2021. [1](#)
- [17] Ligong Han, Yinxiao Li, Han Zhang, Peyman Milanfar, Dimitris Metaxas, and Feng Yang. Svdif: Compact parameter space for diffusion fine-tuning. *arXiv preprint arXiv:2303.11305*, 2023. [1](#), [3](#)
- [18] Ayaan Haque, Matthew Tancik, Alexei A Efros, Aleksander Holynski, and Angjoo Kanazawa. Instruct-nerf2nerf: Editing 3d scenes with instructions. *arXiv preprint arXiv:2303.12789*, 2023. [1](#), [2](#), [3](#), [6](#), [7](#), [8](#)
- [19] Kaiming He, Xiangyu Zhang, Shaoqing Ren, and Jian Sun. Deep residual learning for image recognition. In *Proceedings of the IEEE conference on computer vision and pattern recognition*, pages 770–778, 2016. [4](#)
- [20] Amir Hertz, Ron Mokady, Jay Tenenbaum, Kfir Aberman, Yael Pritch, and Daniel Cohen-Or. Prompt-to-prompt image editing with cross attention control. *arXiv preprint arXiv:2208.01626*, 2022. [3](#)
- [21] Lukas Höllein, Justin Johnson, and Matthias Nießner. Stylemesh: Style transfer for indoor 3d scene reconstructions. In *Proceedings of the IEEE/CVF Conference on Computer Vision and Pattern Recognition*, pages 6198–6208, 2022. [1](#)
- [22] Ferenc Huszár. How (not) to train your generative model: Scheduled sampling, likelihood, adversary? *arXiv preprint arXiv:1511.05101*, 2015. [5](#)
- [23] Mohammad Mahdi Johari, Yann Lepoittevin, and François Fleuret. Geonerf: Generalizing nerf with geometry priors. In *Proceedings of the IEEE/CVF Conference on Computer Vision and Pattern Recognition*, pages 18365–18375, 2022. [4](#)
- [24] Bahjat Kawar, Shiran Zada, Oran Lang, Omer Tov, Huiwen Chang, Tali Dekel, Inbar Mosseri, and Michal Irani. Imagic: Text-based real image editing with diffusion models. In *Proceedings of the IEEE/CVF Conference on Computer Vision and Pattern Recognition*, pages 6007–6017, 2023. [3](#)

- [25] Hyunsu Kim, Gayoung Lee, Yunjey Choi, Jin-Hwa Kim, and Jun-Yan Zhu. 3d-aware blending with generative nerfs. *arXiv preprint arXiv:2302.06608*, 2023. 2, 3
- [26] Mijeong Kim, Seonguk Seo, and Bohyung Han. Infonerf: Ray entropy minimization for few-shot neural volume rendering. In *Proceedings of the IEEE/CVF Conference on Computer Vision and Pattern Recognition*, pages 12912–12921, 2022. 6
- [27] Sosuke Kobayashi, Eiichi Matsumoto, and Vincent Sitzmann. Decomposing nerf for editing via feature field distillation. *arXiv preprint arXiv:2205.15585*, 2022. 1
- [28] Mingi Kwon, Jaeseok Jeong, and Youngjung Uh. Diffusion models already have a semantic latent space. *arXiv preprint arXiv:2210.10960*, 2022. 3
- [29] Junnan Li, Dongxu Li, Silvio Savarese, and Steven Hoi. Blip-2: Bootstrapping language-image pre-training with frozen image encoders and large language models. *arXiv preprint arXiv:2301.12597*, 2023. 6
- [30] Lingjie Liu, Jiatao Gu, Kyaw Zaw Lin, and et al. Neural sparse voxel fields. *NeurIPS 2020*, 33:15651–15663, 2020. 1
- [31] Xihui Liu, Dong Huk Park, Samaneh Azadi, Gong Zhang, Arman Chopikyan, Yuxiao Hu, Humphrey Shi, Anna Rohrbach, and Trevor Darrell. More control for free! image synthesis with semantic diffusion guidance. In *Proceedings of the IEEE/CVF Winter Conference on Applications of Computer Vision*, pages 289–299, 2023. 3
- [32] Yuan Liu, Sida Peng, Lingjie Liu, Qianqian Wang, Peng Wang, Christian Theobalt, Xiaowei Zhou, and Wenping Wang. Neural rays for occlusion-aware image-based rendering. In *Proceedings of the IEEE/CVF Conference on Computer Vision and Pattern Recognition*, pages 7824–7833, 2022. 3, 4
- [33] Ben Mildenhall, Pratul P Srinivasan, Rodrigo Ortiz-Cayon, Nima Khademi Kalantari, Ravi Ramamoorthi, Ren Ng, and Abhishek Kar. Local light field fusion: Practical view synthesis with prescriptive sampling guidelines. *ACM Transactions on Graphics (TOG)*, 38(4):1–14, 2019. 6
- [34] Ben Mildenhall, Pratul P Srinivasan, Matthew Tancik, Jonathan T Barron, Ravi Ramamoorthi, and Ren Ng. Nerf: Representing scenes as neural radiance fields for view synthesis. *Communications of the ACM*, 65(1):99–106, 2021. 6
- [35] Ben Mildenhall, Pratul P Srinivasan, Matthew Tancik, Jonathan T Barron, Ravi Ramamoorthi, and Ren Ng. Nerf: Representing scenes as neural radiance fields for view synthesis. *Communications of the ACM*, 65(1):99–106, 2021. 1, 2, 3, 5
- [36] Thomas Müller, Alex Evans, Christoph Schied, and Alexander Keller. Instant neural graphics primitives with a multiresolution hash encoding. *ACM Transactions on Graphics (ToG)*, 41(4):1–15, 2022. 1
- [37] Michael Oechsle, Songyou Peng, and Andreas Geiger. Unisurf: Unifying neural implicit surfaces and radiance fields for multi-view reconstruction. In *Proceedings of the IEEE/CVF International Conference on Computer Vision*, pages 5589–5599, 2021. 3
- [38] Byong Mok Oh, Max Chen, Julie Dorsey, and Frédo Durand. Image-based modeling and photo editing. In *Proceedings of the 28th annual conference on Computer graphics and interactive techniques*, pages 433–442, 2001. 3
- [39] Keunhong Park, Utkarsh Sinha, Jonathan T Barron, Sofien Bouaziz, Dan B Goldman, Steven M Seitz, and Ricardo Martin-Brualla. Nerfies: Deformable neural radiance fields. In *Proceedings of the IEEE/CVF International Conference on Computer Vision*, pages 5865–5874, 2021. 3
- [40] Ben Poole, Ajay Jain, Jonathan T Barron, and Ben Mildenhall. Dreamfusion: Text-to-3d using 2d diffusion. *arXiv preprint arXiv:2209.14988*, 2022. 3
- [41] Alec Radford, Jong Wook Kim, Chris Hallacy, and et al. Learning transferable visual models from natural language supervision. In *ICML 2021*, pages 8748–8763, 2021. 8
- [42] Aditya Ramesh, Prafulla Dhariwal, Alex Nichol, Casey Chu, and Mark Chen. Hierarchical text-conditional image generation with clip latents. *arXiv preprint arXiv:2204.06125*, 2022. 3
- [43] Robin Rombach, Andreas Blattmann, Dominik Lorenz, Patrick Esser, and Björn Ommer. High-resolution image synthesis with latent diffusion models. In *CVPR 2022*, pages 10684–10695, 2022. 3
- [44] Nataniel Ruiz, Yuanzhen Li, Varun Jampani, Yael Pritch, Michael Rubinstein, and Kfir Aberman. Dreambooth: Fine tuning text-to-image diffusion models for subject-driven generation. In *Proceedings of the IEEE/CVF Conference on Computer Vision and Pattern Recognition*, pages 22500–22510, 2023. 1, 3
- [45] Chitwan Saharia, William Chan, and Saurabh et al. Saxena. Photorealistic text-to-image diffusion models with deep language understanding. *NeurIPS 2022*, 35:36479–36494, 2022. 3
- [46] Mehdi SM Sajjadi, Henning Meyer, Etienne Pot, Urs Bergmann, Klaus Greff, Noha Radwan, Suhani Vora, Mario Lučić, Daniel Duckworth, Alexey Dosovitskiy, et al. Scene representation transformer: Geometry-free novel view synthesis through set-latent scene representations. In *Proceedings of the IEEE/CVF Conference on Computer Vision and Pattern Recognition*, pages 6229–6238, 2022. 2
- [47] Etai Sella, Gal Fiebelman, Peter Hedman, and Hadar Averbuch-Elor. Vox-e: Text-guided voxel editing of 3d objects. *arXiv preprint arXiv:2303.12048*, 2023. 3
- [48] Jascha Sohl-Dickstein, Eric Weiss, Niru Maheswaranathan, and Surya Ganguli. Deep unsupervised learning using nonequilibrium thermodynamics. In *International conference on machine learning*, pages 2256–2265. PMLR, 2015. 3
- [49] Jiaming Song, Chenlin Meng, and Stefano Ermon. Denoising diffusion implicit models. *arXiv preprint arXiv:2010.02502*, 2020. 3
- [50] Kunpeng Song, Ligong Han, Bingchen Liu, Dimitris Metaxas, and Ahmed Elgammal. Diffusion guided domain adaptation of image generators. *arXiv preprint arXiv:2212.04473*, 2022. 3
- [51] Mohammed Suhail, Carlos Esteves, Leonid Sigal, and Ameer Makadia. Generalizable patch-based neural render-

- ing. In *European Conference on Computer Vision*, pages 156–174. Springer, 2022. 3, 5
- [52] Matthew Tancik, Vincent Casser, Xinchun Yan, Sabeek Pradhan, Ben Mildenhall, Pratul P Srinivasan, Jonathan T Barron, and Henrik Kretzschmar. Block-nerf: Scalable large scene neural view synthesis. In *Proceedings of the IEEE/CVF Conference on Computer Vision and Pattern Recognition*, pages 8248–8258, 2022. 1
- [53] Matthew Tancik, Ethan Weber, Evonne Ng, Ruilong Li, Brent Yi, Terrance Wang, Alexander Kristoffersen, Jake Austin, Kamyar Salahi, Abhik Ahuja, et al. Nerfstudio: A modular framework for neural radiance field development. In *ACM SIGGRAPH 2023 Conference Proceedings*, pages 1–12, 2023. 6
- [54] Jiayang Tang, Xiaokang Chen, Jingbo Wang, and Gang Zeng. Compressible-composable nerf via rank-residual decomposition. *Advances in Neural Information Processing Systems*, 35:14798–14809, 2022. 1
- [55] Can Wang, Menglei Chai, Mingming He, and et al. Clip-nerf: Text-and-image driven manipulation of neural radiance fields. In *CVPR 2022*, pages 3835–3844, 2022. 1, 7
- [56] Chen Wang, Xian Wu, Yuan-Chen Guo, and et al. Nerf-sr: High quality neural radiance fields using supersampling. In *ACM MM 2022*, pages 6445–6454, 2022. 1
- [57] Can Wang, Ruixiang Jiang, Menglei Chai, Mingming He, Dongdong Chen, and Jing Liao. Nerf-art: Text-driven neural radiance fields stylization. *IEEE Transactions on Visualization and Computer Graphics*, 2023. 2, 3, 6, 7
- [58] Peng Wang, Lingjie Liu, Yuan Liu, Christian Theobalt, Taku Komura, and Wenping Wang. Neus: Learning neural implicit surfaces by volume rendering for multi-view reconstruction. *arXiv preprint arXiv:2106.10689*, 2021. 1, 3
- [59] Peihao Wang, Xuxi Chen, Tianlong Chen, Subhashini Venugopalan, Zhangyang Wang, et al. Is attention all nerf needs? *arXiv preprint arXiv:2207.13298*, 2022. 2, 3, 4
- [60] Qianqian Wang, Zhicheng Wang, Kyle Genova, Pratul P Srinivasan, Howard Zhou, Jonathan T Barron, Ricardo Martin-Brualla, Noah Snavely, and Thomas Funkhouser. Ibrnet: Learning multi-view image-based rendering. In *Proceedings of the IEEE/CVF Conference on Computer Vision and Pattern Recognition*, pages 4690–4699, 2021. 3, 6
- [61] Suttisak Wizatdwongsa, Pakkapon Phongthawee, Jiraphon Yenphraphai, and Supasorn Suwajanakorn. Nex: Real-time view synthesis with neural basis expansion. In *Proceedings of the IEEE/CVF Conference on Computer Vision and Pattern Recognition*, pages 8534–8543, 2021. 3
- [62] Tao Xu, Pengchuan Zhang, Qiuyuan Huang, and et al. AttnGAN: Fine-grained text to image generation with attentional generative adversarial networks. In *CVPR 2018*, pages 1316–1324, 2018. 3
- [63] Serin Yang, Hyunmin Hwang, and Jong Chul Ye. Zero-shot contrastive loss for text-guided diffusion image style transfer. *arXiv preprint arXiv:2303.08622*, 2023. 3
- [64] Zhenpei Yang, Zhile Ren, Qi Shan, and Qixing Huang. Mvs2d: Efficient multi-view stereo via attention-driven 2d convolutions. In *Proceedings of the IEEE/CVF Conference on Computer Vision and Pattern Recognition*, pages 8574–8584, 2022. 5
- [65] Alex Yu, Vickie Ye, Matthew Tancik, and Angjoo Kanazawa. pixelnerf: Neural radiance fields from one or few images. In *Proceedings of the IEEE/CVF Conference on Computer Vision and Pattern Recognition*, pages 4578–4587, 2021. 3
- [66] Han Zhang, Jing Yu Koh, Jason Baldridge, Honglak Lee, and Yinfei Yang. Cross-modal contrastive learning for text-to-image generation. In *Proceedings of the IEEE/CVF conference on computer vision and pattern recognition*, pages 833–842, 2021. 3
- [67] Lvmin Zhang, Anyi Rao, and Maneesh Agrawala. Adding conditional control to text-to-image diffusion models. In *Proceedings of the IEEE/CVF International Conference on Computer Vision*, pages 3836–3847, 2023. 3
- [68] Jingyu Zhuang, Chen Wang, Lingjie Liu, Liang Lin, and Guanbin Li. Dreameditor: Text-driven 3d scene editing with neural fields. *arXiv preprint arXiv:2306.13455*, 2023. 1, 2, 3, 7